Generative AI-Powered Inverse Design for Tailored Narrowband Molecular Emitters

Mianzhi Pan[1,4,5†], Tianhao Tan[2,3†], Yawen Ouyang[1†], Qian Jin[2,3], Yougang Chu[4], Wei-Ying Ma[1], Jianbing Zhang[4,5*], Lian Duan[2,3*], Dong Wang[2,3*], Hao Zhou[1*]

[1]Institute of AI Industry Research(AIR), Tsinghua University, Beijing, China.
[2]Laboratory of Flexible Electronics Technology, Tsinghua University, Beijing, China.
[3]MOE Key Laboratory of Organic OptoElectronics and Molecular Engineering, Department of Chemistry, Tsinghua University, Beijing, China.
[4]National Key Laboratory for Novel Software Technology, Nanjing University, Nanjing, Jiangsu, China.
[5]School of Artificial Intelligence, Nanjing University, Nanjing, Jiangsu, China.

E-mail: panmz@smail.nju.edu.cn; tth19@mails.tsinghua.edu.cn; dong913@mail.tsinghua.edu.cn; zhouhao@air.tsinghua.edu.cn;
[†]These authors contributed equally to this work.

Abstract

In organic displays, developing molecules that produce a broad color gamut with exceptional color purity is of critical importance. AI-assisted molecular screening can expedite the design process of emission molecules. However, the efficiency of current methodologies is constrained by their limited candidate pools and poor hit rates. Here we present MEMOS, a cutting-edge molecular generation framework that, through Markov molecular sampling techniques, facilitates the targeted inverse design of molecules across a nearly boundless chemical space, tailored to emit the narrow spectral bands associated with desired colors. Notably, by employing a self-improving iterative process, MEMOS achieves an impressive hit rate of up to 80%. Our method showcases the pioneering capability to rapidly navigate through millions of molecular possibilities, efficiently pinpointing thousands of high-potential candidates within a 24-hour period. This breakthrough accelerates the design of novel organic luminescent materials, setting the stage for the advancement of the next generation of high-quality organic displays.

Introduction

Organic light-emitting diodes (OLEDs) have emerged as highly promising light-emitting devices for applications in lighting and displays, owing to their rapid response, wide viewing angles, and flexibility. Color purity is a critical attribute for emitters, as it directly influences color deviation and the realism of the display. Typically, the color purity of an emitter is assessed by the full width at half-maximum (FWHM) of its emission spectrum. Minimizing the FWHM is essential for achieving color coordinates that are closer to the outer boundary of the color space, thereby ensuring a more accurate color representation.

Recently, a novel class of emitter molecules with narrowband emission, known as multiple resonance thermally activated delayed fluorescent (MR-TADF) materials, has been introduced [1]. These materials leverage resonance effects to confine frontier orbitals to specific atoms by incorporating elements with complementary electronegativity, such as boron and nitrogen, at the ortho- or para-positions of rigid conjugated rings. This approach not only effectively separates the HOMO and LUMO orbitals, endowing the molecule with excellent thermally activated delayed fluorescence properties, but also

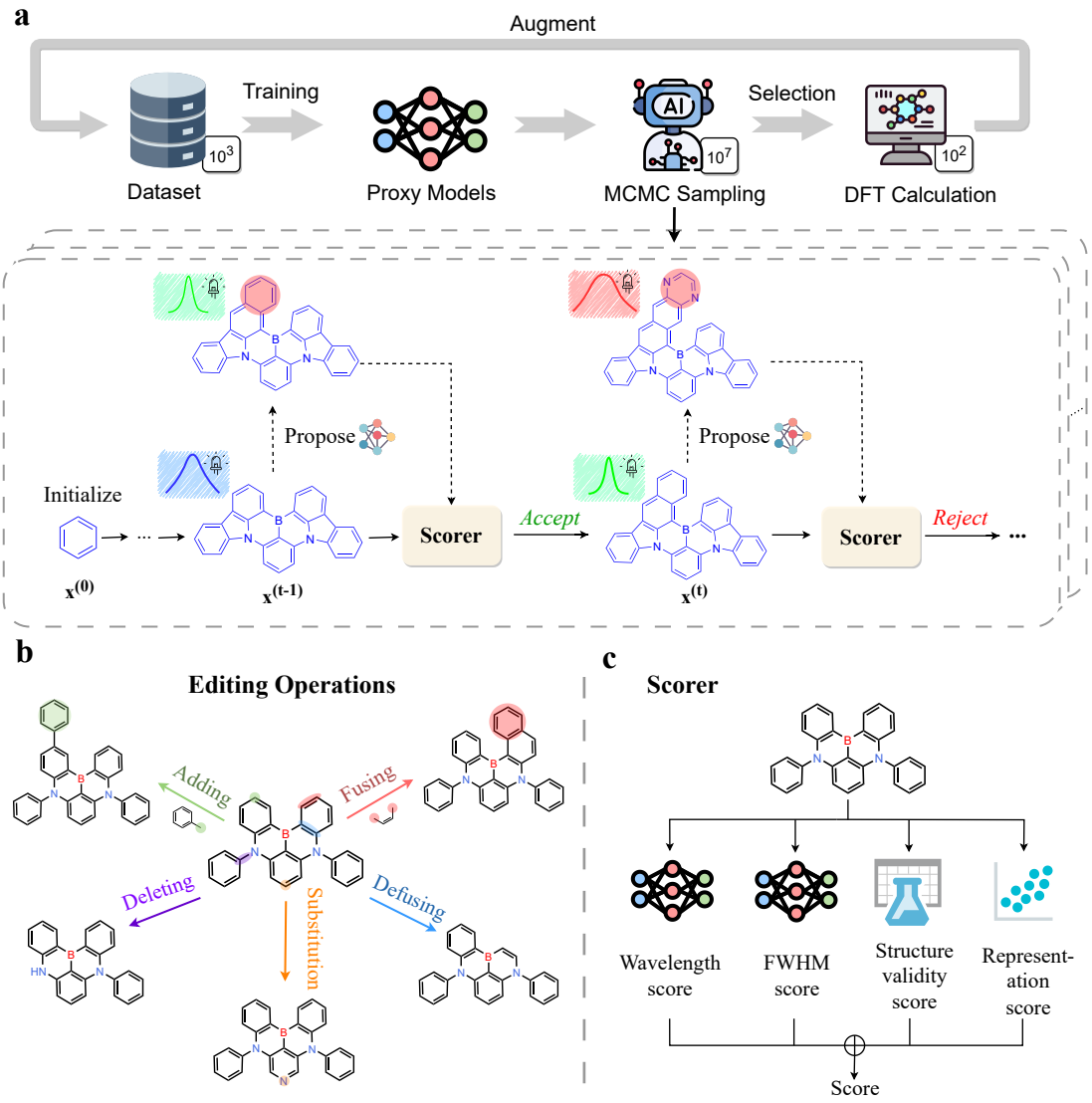

Fig. 1 (a) Schematic overview of MEMOS: a self-improving OLED molecule design system utilizing Markov Chain Monte Carlo (MCMC) sampling. (b) Schematic diagram of all molecular editing operations. (c) Schematic diagram of the scorer used in MCMC sampling.

curtails the deformation of the excited state and reduces electron-vibrational coupling, leading to a narrowed emission profile [2, 3]. To date, multiple resonance strategies have yielded narrowband emitters with the narrowest reported emission peak exhibiting an FWHM of just 13 nm in the blue, 14 nm in the green and 21 nm in the red spectral regions. [4–10]. However, the rarity of molecules that exhibit narrowband emissions in the long-wavelength regions poses a significant challenge. Most molecules, especially those emitting in the green and red spectra, still display emission peaks with an FWHM exceeding 20 nm. This scarcity of high-performance red and green emitters has become a critical bottleneck in the advancement of OLED materials discovery.

Traditionally, designing ideal luminescent molecules involves a laborious cycle of extensive synthesis and validation, which often incurs significant costs due to the trial-and-error nature of the approach. High-throughput virtual screening (HTVS) complemented by theoretical calculations is considered a more cost-effective approach for material discovery [11]. Nevertheless, accurately predicting the emission peaks and FWHM for a vast array of molecular spectra remains challenging due to the computationally intensive task of calculating Hessian matrices for excited states. Machine learning (ML) methods, which establish structure-property relationships to enable rapid property prediction

without the need for extensive theoretical calculations, have substantially expedited the HTVS process [12–17]. These methods have been applied to screen for organic emitters that offer high PLQY, a wide color gamut, or high color purity [18–20].

Despite these advancements, the efficiency of ML-accelerated HTVS is still bounded by several inherent limitations. First, it relies on a limited set of pre-designed candidate molecules, which only represent a small fraction of the vast molecular space. Second, the processes of molecule generation and screening are separate, leading to a low hit rate and necessitating more time investment. As a result, these approaches hinder the comprehensive and efficient exploration of the chemical space. Therefore, there is an urgent call for a more integrated methodology capable of freely navigating the vast chemical space and optimizing molecules in real-time through feedback on the molecules generated.

In this study, we present **M**arkov **E**mission **MO**lecular **S**ampling (**MEMOS**), a framework designed for efficient multi-objective inverse design of luminescent molecules. Inspired by the success of Markov chain Monte Carlo (MCMC) sampling method in generating text [21] and drug-like molecules [22], MEMOS adapts MCMC sampling for the organic light-emitting context by integrating specialized molecular editing operations and scoring functions.

In the MEMOS framework, candidate molecules are generated at each time step through one editing operation applied to the molecules from the preceding step. This approach enables the exploration of an almost limitless chemical space, free from the constraints of limited candidate pools. The acceptance of the generated molecules is determined by their property scores, such as emission wavelength and FWHM. This design procedure allows the properties of the sampled molecules to be guided toward the target values. Leveraging a self-improving discovery cycle, the accuracy of our proxy models can be significantly enhanced, achieving a high hit rate of up to 70% for emission wavelength and 80% for FWHM. This, in turn, facilitates the efficient inverse design of MR fluorescent molecules.

Utilizing MEMOS to design molecules for red, green, and blue light emission, we have successfully created a diverse array of molecules with finely tunable colors and FWHM reaching 13 nm in the blue, 15.5 nm in the green and 20 nm in the red spectral regions. The CIE color coordinates of these molecules closely align with the Rec. 2020 [23] standard, holding great promise for expanding the color gamut and achieving ultra-high-definition displays. Our approach can markedly improve the efficiency of molecule design and demonstrates the potential of AI in venturing into the realm of cutting-edge narrow-emission molecules.

Results and Discussion

Overview of MEMOS

Discovering molecules that display the desired color and high color purity is a formidable challenge due to the immense molecular space. Current ML-accelerated HTVS methods [18, 20] have endeavored to explore the molecular space by empirically modifying existing molecules and systematically enumerating candidate molecules, a process that is both inefficient and computationally demanding.

In contrast, we have developed a novel framework, MEMOS, grounded in MCMC sampling to design molecules with targeted optical properties. **Figure 1 (a)** depicts the workflow of MEMOS: First, the MCMC sampling process continuously generates candidate molecules from a seed molecule by modifying those from preceding steps with five molecular graph editing operations (**Figure 1 (b)**): fragment *Adding* and *Deleting*, ring *Fusing* and *Defusing*, and atom *Substitution*. Proposals for these operations are represented by message-passing neural networks (MPNNs) [24], which are adaptively trained throughout the sampling. Subsequently, proxy models predict the emission wavelength and FWHM of the sampled molecules. The acceptance of the newly generated molecule is determined based on its score on the objective function,(**Figure 1 (c)**) which encompasses structural and representational rationality, wavelength, and color purity. Density functional theory (DFT) is then applied to ascertain the precise optical properties of the top-k generated molecules. Lastly, these data are used to iteratively refine the proxy model, creating a self-improving loop for the design of target molecules.

As the cornerstone of our framework, the MCMC sampling method with a simulated annealing [25] scheme is employed to navigate the chemical space in search of molecules with desired properties. Specifically, it constructs a Markov Chain within the chemical space where each state corresponds to a molecule, and the Markov Chain's equilibrium distribution is aligned with the target distribution [26,

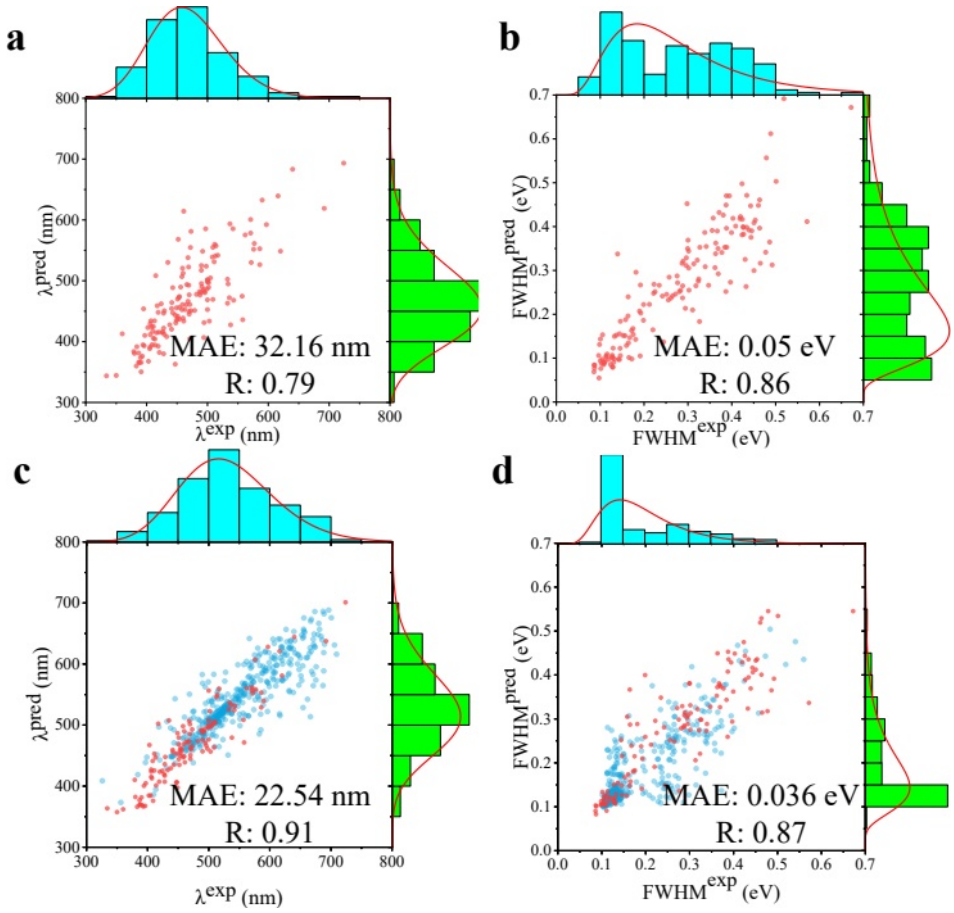

Fig. 2 Mean absolute error (MAE) and distribution of labels on test set against the prediction of initial proxy models for (a) emission peak wavelengths, (b) the FWHM of the emission spectrum, and prediction of adapted proxy models in the last iteration for (c) emission peak wavelengths, (d) the FWHM of the emission spectrum. Data from the initial experiment dataset are marked in red, while newly added DFT-calculated data are highlighted in blue.

27]. Therefore, with an increasing number of sampling steps, the initial molecule can progressively enhance its objective function score, ultimately achieving the desired properties.

To transform between molecules, the original MARS approach [22] considers fragment *Adding* and *Deleting*. However, relying solely on these operations is insufficient for effectively exploring the molecular space, since organic light-emitting molecules typically feature multiple fused ring structures. Moreover, simply adding single bonds through the *Adding* operation may lead to significant long-range charge transfer, which is not conducive to the sampling of narrow emission molecules. To address this limitation, MEMOS expands the operation set to include ring *Fusing* and *Defusing*, as well as heteroatom *Substitution*. With these additional operations, MEMOS can explore more than 100 novel molecules per step. Furthermore, up to 300 Markov chains, each undergoing 1500 steps, can be established and evolved on a single NVIDIA RTX 3090 Graph Processing Unit (GPU) within a day. Consequently, MEMOS can uncover ∼45,000,000 molecules in a single day, thereby facilitating a more efficient exploration of a broader, almost infinite chemical space compared to traditional HTVS approaches. This enables the generation of a more diverse set of candidate molecules and facilitates the efficient inverse design of narrowband emitters.

Proxy model performance in optical property prediction

The accurate prediction of molecular properties is essential in machine-learning applications. Uni-Mol [28] as a pre-training model in particular, has demonstrated remarkable proficiency in forecasting the optical properties of organic molecules [18]. Based on the Transformer [29] architecture, Uni-Mol takes 3D molecular conformations as input and leverages its pre-training on a vast array of molecular conformations to generate high-quality molecular representations. Upon fine-tuning, Uni-Mol exhibits

exceptional performance across a range of downstream tasks. Consequently, we utilize Uni-Mol as the proxy model to predict the emission peaks wavelengths and spectral FWHM of molecules. We have developed separate models for each property, each comprising a Uni-Mol backbone complemented by a multilayer perceptron (MLP). The MLP transforms the vector output from Uni-Mol into a scalar value, which represents the final prediction for each property. **Figure 2 (a-b)** illustrated the performance of our models on the initially collected dataset.(see **Methods**) These results are based on the models' predictions on a predefined test set, which is distinct from the training set. Overall, both models have been successfully trained using our meticulously curated dataset. The correlation coefficient (R) and mean absolute error (MAE) are 0.79 and 32.16 nm for the emission peak wavelength, and 0.86 and 0.05 eV for the FWHM, respectively. These metrics indicate that the models are capable of accurately estimating these two molecular properties, which in turn enables their use in informing the subsequent molecular sampling process.

Iteratively adapting to the MEMOS-explored chemical space

One challenge in material design arises when proxy models, used in designing algorithms, encounter novel chemical spaces that differ from the training data [30, 31], leading to a degradation of the quality of the generated molecules, known as out-of-distribution (OOD) problems [32, 33]. To address this issue, Fannjiang and Listgarten [34] propose iterative retraining of proxy models by focusing on previously high-scoring molecules. Similarly, we suggest iteratively updating the proxy models with newly generated molecules, allowing the models to adapt to the novel chemical space explored by MEMOS.

As illustrated in **Figure 1**, the top-k molecules are selected as the final sampled candidates and labeled based on the results from DFT calculations. These labeled molecules are then integrated into the dataset to enhance the training of the proxy models. The updated models are employed in the subsequent sampling phase, thus creating a self-improving loop. With each iteration, the proxy models become capable of predicting the properties of a broader range of molecules. **Figure 2 (c-d)** demonstrate that the refined models achieve superior accuracy in predictions on test datasets that include the initial test data and the sampled molecules. Consequently, the hit rate of MEMOS has notably increased during the self-improving loop. **Figure 3 (a-b)** shows the shift in property distributions of the sampled molecules over successive iterations. Here, we are targeting green light molecules. The iterative process of the model has resulted in an increasing number of sampled molecules emitting within the 525 $\pm$ 25 nm range and with FWHM below 0.125 eV. By the fifth iteration, approximately 70% of sampled molecules emit colors that align with the target expectation (525 $\pm$ 25 nm), and nearly 80% meet the target criterion for FWHM values (<0.125 eV). These findings demonstrate that MEMOS efficiently samples molecules for narrowband green light emission.

The rising hit rate indicates that the proxy model is progressively adapting to the novel chemical space explored by MEMOS. We employ t-SNE [35] to visualize the distribution of sampled molecules in chemical space across iterations. As depicted in **Figure 3 (c)**, initially, the sampled molecules cluster at the outskirts of the distribution of experimental molecules. Due to the scarcity of data in this area, the reliability of the predicted properties is relatively low, leading to a low hit rate of MEMOS. As the iterations progress, MEMOS gradually extends its exploration to a wider chemical space. The incorporation of this data into the dataset enhances the representation of the chemical space, thereby improving the model's generalization capability. Consequently, the predictions become more trustworthy, and the sampling hit rate steadily increases. After five iterations, almost all newly sampled molecules are situated within the chemical space covered by the dataset. This suggests that, after several iterations, our model effectively samples from a sufficiently expansive space to thoroughly explore the structures of MR molecules emitting green light.

In addition to optical properties, synthesis accessibility is a critical metric for evaluating the practical applicability of organic light-emitting molecules. The synthesis accessibility of green light-emitting molecules sampled from different iterations was evaluated using fragment spatial and stereoselective-based synthesis accessibility scores (SAscore) [36], which are integrated into the rdkit package [37]. As shown in **Figure 3 (d)**, there is a trend of decreasing synthesis accessibility sGcores over each iteration. This trend may suggest that the structures of sampled molecules are evolving towards greater rationality and simplicity, with a reduction in the presence of unconventional structural elements. After five iterations, around 50% of the molecules have synthesis accessibility scores below 3.5, suggesting

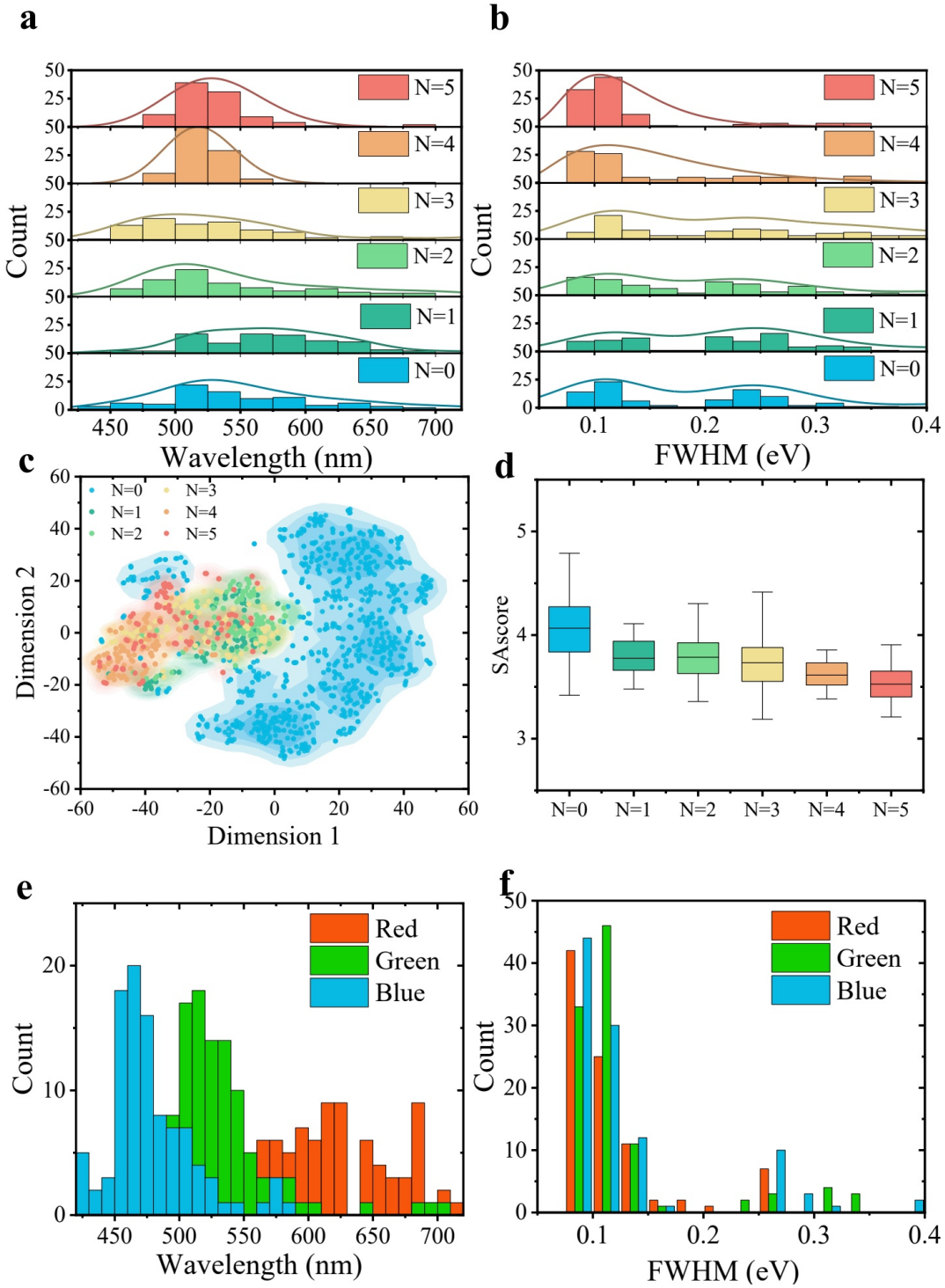

Fig. 3 (a) Distribution of emission peak wavelengths for sampled molecules across different iterative batches. (b) Distribution of emission FWHM for sampled molecules across different iterative batches. (c) Distribution of sampled molecules from different iterative batches within chemical space. (d) Boxplot of synthetic accessibility scores for sampled molecules across different iterative batches. The upper and lower boundaries of the boxes represent the first and third quartiles, respectively; the whiskers indicate 1.5 times the standard deviation, and the median is denoted by a center line. (e) Distribution of emission peak wavelengths for sampled molecules intended for RGB light emission in the fifth iteration. (f) Distribution of emission FWHM for sampled molecules targeting RGB light emission in the fifth iteration.

that these candidate molecules could be more readily synthesized and are promising candidates for use in OLEDs.

Candidate molecules discovery

Using the iteratively adapted proxy models, we have successfully sampled narrowband molecules across the blue, green, and red light spectra, thereby facilitating the efficient inverse design of narrowband molecules for any targeted light color (**Figure 3 e-f**). During the sampling process, several well-known emitters such as CzBN, CzBO, γ-Cb-B, Phenanthrene, Py-Cz, and InBN [5, 38–41], were recovered from basic fragments that could not be further divided by deleting or defusing, using our designed action. using our approach. Among these, CzBN, CzBO, γ-Cb-B, and InBN are blue-emitting MR molecules, with emission peak positions at 477 nm, 445 nm, 460 nm, and 475 nm. The FWHM for these emitters is 25 nm, 26 nm, 23 nm, and 23 nm, respectively. This demonstrates that the vocabulary and actions within MEMOS are sufficient for constructing potential high-performance molecules. Structures similar to more complex molecules, such as BN-ICZ,[42] which has an emission peak at 521 nm and FWHM of 23 nm, or BTC-BNCz[43] which has an emission peak at 488 nm and FWHM of 23 nm can be recovered during the sampling process, differing by only one substituent. However, achieving complete consistency in recovery still requires the addition of extra constraints, such as symmetry and reactivity. The hit rate for sampling red light-emitting molecules is somewhat lower, and the wavelength distributions are broader compared to those of blue and green light-emitting molecules. This discrepancy is likely attributable to the smaller number of reported red light-emitting molecules in the dataset.

Employing MEMOS, we can sample thousands of candidate molecules daily that meet our criteria for color and FWHM, thereby efficiently expanding the array of known MR materials. Those sampled molecules fall into distinct categories including boron-nitrogen based, boron-oxygen based,carbonyl-nitrogen based, and indolo[3,2,1-jk]carbazole (ICZ) based types, each exhibiting a variety of novel and unique structures. These new structures provide valuable insights for the exploration and design of advanced materials. Typical structures of the sampled red, green, and blue light-emitting molecules with outstanding performance are illustrated in **Figure 4**.

Beyond exhibiting innovative structures, the sampled molecules also demonstrate excellent performance. Our approach precisely tunes the emission wavelength of the molecules to the target values through peripheral substituent modifications and heteroatom incorporation. Meanwhile, the sampled molecules exhibit high oscillator strengths, which favor enhanced luminous efficiency. **Figure 3 (b,f)** and **Figure 2 (d)** both show that the FWHM of the majority of the sampled molecules falls within the range of 0.075-0.125 eV, with a scarcity of molecules exhibiting FWHM values below 0.075 eV. As illustrated in **Figure 4**, the narrowest FWHM among these sampled molecules can reach 20 nm/76.7 meV for red, 15.5 nm/74.1 meV for green, and 13 nm/74.4 meV for blue emissions, respectively, which rival the narrowest FWHM observed in existing molecular entities. These results suggest a lower bound for the FWHM of current-type MR molecules and demonstrate the ability of our method to define the limits of molecular properties.

To precisely tune the optical properties of the molecules to meet our target specifications, our model has progressively adopted molecular design strategies from the dataset during the MEMOS sampling process, without preset manual adjustments. For instance, the model implemented the double boron embedded strategies [8, 45], which strategically incorporate additional boron(B) or nitrogen(N) atom at the meta/para positions of the existing boron atom. This incorporation effectively modulates the strengths of intramolecular charge transfer and enhances the multi resonance effect on the central ring, thereby fine-tuning the spectral color output and narrowing the emission peak. For example, compared to molecules fused to benzene rings without additional B/N incorporation, the spectra of the highlighted double boron embedded molecules in **Figure 4** exhibit a pronounced blue shift over 100 nm, changing from red emission to our desired green emission while the FWHM narrows to nearly 10 nm.(Figure S8) This indicates that the model has learned underlying patterns from the training data, strategically incorporating heteroatoms to precisely tune molecular properties and meet our requirements.

Electron-hole analysis [46] reveals that the sampled molecules display pronounced short-range charge transfer (SR-CT) characteristics(**Figure 5** a-c), effectively mitigating electron vibtational coupling and consequently narrows the emission peak. By systematic modular charge transfer characteristics, these model-designed molecules have achieved a narrowed emission profile along with a

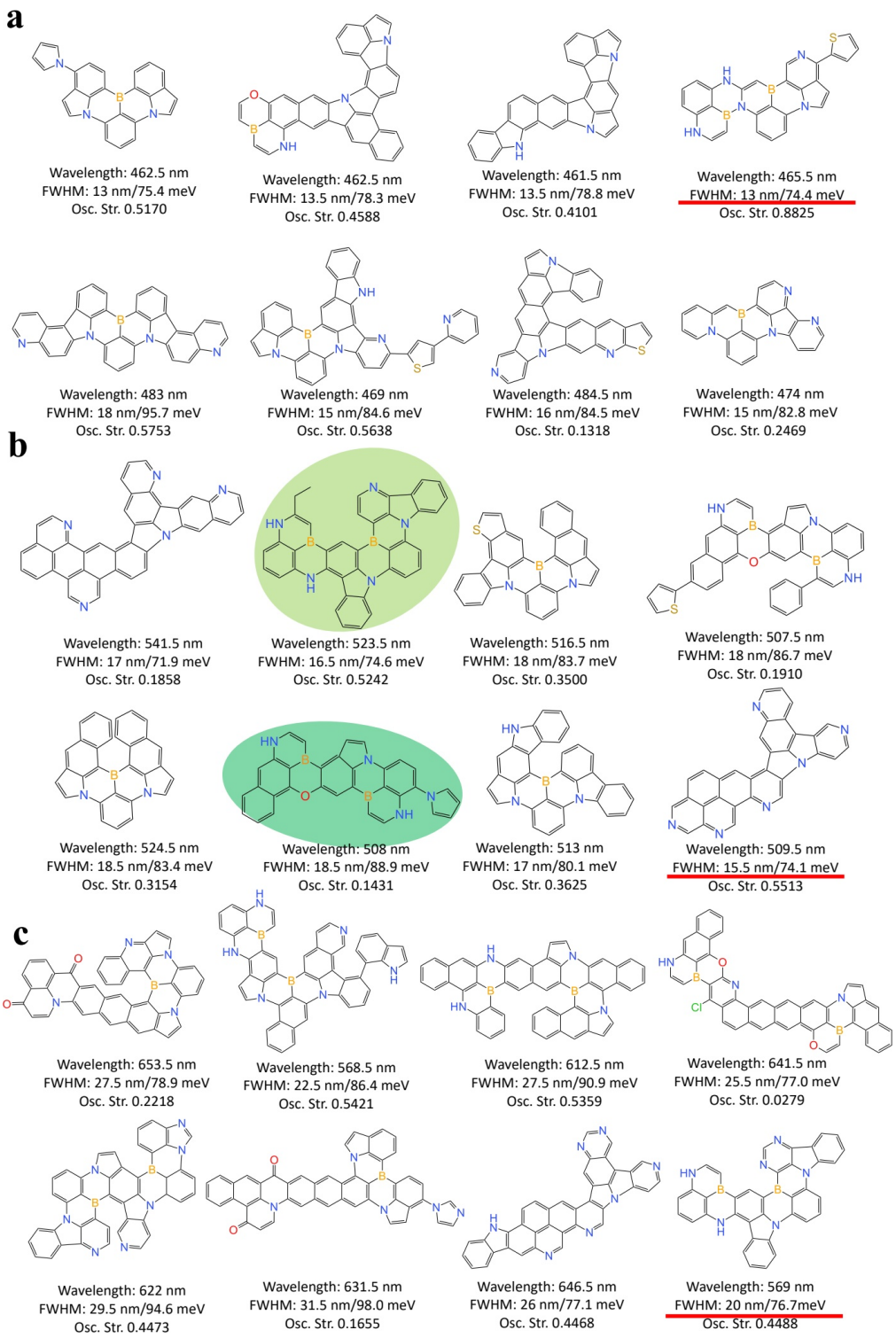

Fig. 4 Typical structures of the sampled candidate molecules for (a) blue, (b) green, and (c) red emissions, with the corresponding emission wavelengths, FWHM, and oscillator strengths listed. The narrowest FWHM in each emission color are indicated by red underlines. Molecules exemplifying the application of double boron embedded design strategy is highlighted.

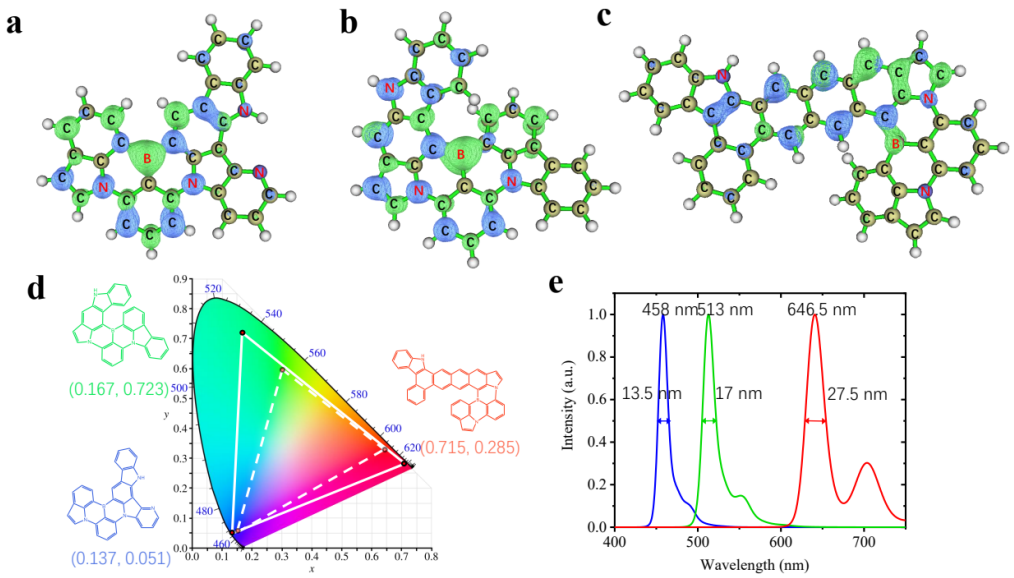

Fig. 5 Isosurfaces of hole and electron distribution for the screened-out candidate molecules of(a) blue (b) green (c) red emissions. Blue and green isosurfaces represent hole and electron distributions respectively. Electron-hole analyses were performed utilizing the Multiwfn software [44]. (d) The color space constructed using the three candidate molecules demarcated by solid lines, compared to the standard sRGB color space demarcated by dashed lines, with the CIE coordinates of candidates listed. (e) Theoretical calculated emission spectra for the three candidates, including the emission wavelength and FWHM values.

spectrum of tunable emission colors. Furthermore, the SR-CT features also ensure substantial orbital overlap between the HOMO and LUMO, thereby endowing the significant oscillator strength.

Beyond the narrow FWHM of the sampled molecules, our targeted inverse design approach, directed by specific wavelength criteria, has fine-tuned the CIE color coordinates of the molecules. From our sampled pool, we identified candidates capable of constructing a wider color gamut that not only exceeds the range of the regular sRGB color space but also closely aligns with the Rec.2020 [23] standard, with CIE coordinates of (0.137, 0.051) for blue, (0.167, 0.723) for green, and (0.715, 0.285) for red(**Figure 5 d-e**).

Conclusion

By combining MCMC sampling with property prediction models, we have streamlined the inverse design of molecules capable of narrowband emissions across the entire spectrum of wavelengths. This integration facilitates a more efficient exploration of the expansive chemical space compared to conventional HTVS approaches. Through a self-improving iterative process, the novel chemical space investigated by MEMOS can be progressively refined by the proxy model, achieving hit rates of 70% for emission peak wavelengths and 80% for the FWHM. Our model uncovers design strategies from existing molecules, systematically modulates the charge transfer characteristics of the model-designed molecules, successfully narrows their emission spectra, and fine-tunes their molecular emission to the target color. The FWHM of the sampled molecules is recorded at 27.5 nm/81.6 meV for red, 17 nm/80.1 meV for green, and 13.5 nm/79.8 meV for blue emissions. These characteristics enable our sampled molecules to contribute to the extensive color gamut required for ultra-high-definition displays. With the integration of enhanced vocabularies and editing operations, our approach can delve into a broader chemical space and uncover molecules with even narrower FWHM. Furthermore, our approach is readily adaptable for the concurrent multi-objective optimization of desirable attributes, such as luminescence efficiency, stability, and fluorescence lifetime. Our findings demonstrate the potential to construct a broad color gamut and are expected to accelerate the development and discovery of novel organic luminescent materials.

Methods

Dataset construction and proxy models training

The initial dataset was constructed by collecting molecules with multiple resonance structures and narrow spectral profiles, as reported in the literature. To minimize the impact of other factors on the spectral data, the emission peak wavelength (measured in nm) and FWHM (measured in eV) of the emission spectra in dichloromethane or toluene solutions were used as labels. Furthermore, we expanded the dataset by including molecules from the dataset reported by Park et. al. [47] that exhibited an FWHM below 100 nm in either dichloromethane or toluene solutions. The final dataset consisted of 811 molecules, with 320 of them possessing multiple resonance structure characteristics.

The Uni-Mol models were fine-tuned using this curated dataset. We trained two separate models to predict each of these properties individually. Both properties were normalized to adhere to a standard normal distribution. The entire dataset was randomly partitioned into training and validation sets in a 4:1 ratio. Before input into Uni-Mol, all molecules were converted into a 3D conformation using the Experimental-Torsion Basic Knowledge Distance Geometry (ETKDG) [48] algorithm and optimized with the MMFF94 force field [49] by the RDKit program. During training, we utilized the Adam optimizer and employed mean squared error (MSE) as the loss function. Each model was trained for 100 epochs, and the training process was terminated if the validation MSE did not show improvement for 10 consecutive epochs. The batch size was set to 32, and the learning rate was fixed at 1×10^{-4}. The remaining training hyperparameters were consistent with the pre-training procedure of Uni-Mol, as detailed in the original paper [28].

Spectra calculation

During the active learning phase, the DFT-calculated emission spectra of the sampled molecules were integrated into the dataset. The emission spectrum was obtained by computing the thermal vibration correlation function (TVCF) using the MOlecular MAterials Property Prediction Package (MOMAP) [50], without accounting for the Herzberg-Teller effect and Duschinsky rotation.

Structural optimizations for both the ground and excited states, along with electronic energy and frequency analyses, were conducted at the B3LYP-D3(BJ)/6-31g* level of theory using the Gaussian 16 package [51]. Solvent effects were taken into consideration through the Polarizable Continuum Model using the Integral Equation Formalism (IEFPCM), with the solvent's volume and dielectric constant set according to the properties of toluene.

To further mitigate the impact of discrepancies between experimental and computational spectra on model training, the calculated emission wavelengths and FWHM were calibrated based on a linear regression relationship prior to model training.

Molecular sampling

Sampling objective. The sampling objective of MEMOS is defined as:

$$\pi(x) = S_{\text{rep}}(x) + S_{\text{struct}}(x) + S_{\text{wave}}(x) + S_{\text{FWHM}}(x)$$

Here, $\pi(x)$ represents the objective function of molecule x and also serves as an unnormalized probability distribution over the chemical space from which we aim to sample. The four objective functions of the RHS are formulated as follows:

- Molecular representation constraint: A challenge in material design is that the proxy models may be less reliable for molecules distant from the training data. To mitigate this issue, we imposed a constraint on the proximity of sampled molecules to the training data X_{train} within the representation space of Uni-Mol. The corresponding score function is defined as $S_{\text{rep}}(x) = 1/\max(d(x, X_{\text{train}}), D)$, where D is a threshold and $d(x, X_{\text{train}})$ calculates the distance between x and X_{train}. In practice, we use the Euclidean distance between x and the center of X_{train}. S_{rep} encourages the sampling of molecules that are within a distance of D from the training data, hence ensuring the reliability of model predictions.

- Molecular structure validity: Valid OLED molecules are subject to various structural constraints. To address this, we empirically limited the topology of molecular graphs and introduced a score function, $S_{\text{struct}}(x) = \exp(-N(x))$, where $N(x)$ represents the count of unfavorable substructures in x, such as -BH.
- Emission peak wavelength: The score function for the emission peak wavelength (in nm) is defined as:
$$S_{\text{wave}}(x) = \frac{50 - \min\big(|f_{\text{wave}}(x) - W_{\text{target}}|, 50\big)}{50}$$
where $f_{\text{wave}}(\cdot)$ is the wavelength predictor and W_{target} is the target wavelength.
- FWHM of the emission spectrum: The score function for the spectral FWHM (in eV) is given by
$$S_{\text{FWHM}}(x) = \frac{0.4 - \min\big(|f_{\text{FWHM}}(x)|, 0.4\big)}{0.4}$$
where $f_{\text{FWHM}}(\cdot)$ is the FWHM predictor.

All other scores are set to zero when $S_{\text{rep}}(x) \neq 1/D$, indicating that molecule x is significantly distant from the training data, which is not pertinent to our analysis.

Molecular editing operations. To transform one molecule into another, we considered five molecular editing operations based on the molecular graph, as illustrated in **Figure 1 (b)**. Specifically, the *Adding* and *Fusing* operations involve expanding the molecule by attaching a structure from predefined vocabularies. Conversely, the *Deleting* and *Defusing* operations serve as the inverse of *Adding* and *Fusing*, respectively. Finally, the *Substitution* operation converts a valency-permissive aromatic carbon (or nitrogen) to nitrogen (or carbon).

Parameterizing proposal distributions with MPNNs. All proposal distributions for the editing operations were parameterized using Message Passing Neural Networks (MPNNs), a type of Graph Neural Networks (GNNs) that iteratively updates node features by exchanging messages with their neighboring nodes. Specifically, we employ graph convolutions as the message-passing function. Detailed MPNNs' architecture is displayed in **Figure S6**. The MPNNs are trained in a self-adaptive manner with samples from MCMC, which can increase the likelihood of generating high-quality proposals and thus enhance the efficiency of searching the chemical space.

Molecular sampling process. During each sampling process, 300 trajectories were established, originating from randomly selected seed molecules. Each trajectory undergoes 1,500 editing steps. At each time step, we randomly selected an operation with a fixed probability. Once the operation is determined, a molecule x is edited according to the corresponding proposal distributions, yielding a new molecule x'. We decided whether to accept x' with a probability of $\min\{1, \pi^{\alpha}(\mathrm{x}')/\pi^{\alpha}(\mathrm{x})\}$, where $\alpha = 1/0.95^{\lfloor t/5 \rfloor}$. t is the index of the sampling time step. Finally, molecules from the last 200 steps were collected, and the top-100 unique molecules with the highest scores were selected for DFT calculation.

Data & Code availability

We will release the code and data associated with this study upon acceptance of the manuscript for publication.

References

[1] Hatakeyama, T. *et al.* Ultrapure blue thermally activated delayed fluorescence molecules: Efficient HOMO-LUMO separation by the multiple resonance effect. *Adv. Mater.* **28**, 2777–2781 (2016).

[2] Teng, J.-M., Wang, Y.-F. & Chen, C.-F. Recent progress of narrowband tadf emitters and their applications in OLEDs. *J. Mater. Chem. C* **8**, 11340–11353 (2020).

[3] Kim, H. J. & Yasuda, T. Narrowband emissive thermally activated delayed fluorescence materials. *Adv. Opt. Mater.* **10**, 2201714 (2022).

[4] Kondo, Y. *et al.* Narrowband deep-blue organic light-emitting diode featuring an organoboron-based emitter. *Nat. Photonics* **13**, 678–682 (2019).

[5] Xu, Y. *et al.* Molecular-structure and device-configuration optimizations toward highly efficient green electroluminescence with narrowband emission and high color purity. *Adv. Opt. Mater.* **8**, 1902142 (2020).

[6] Zhang, Y. *et al.* Multi-resonance induced thermally activated delayed fluorophores for narrowband green OLEDs. *Angew. Chem. Int. Ed.* **58**, 16912–16917 (2019).

[7] Cheng, Y. C. *et al.* A highly twisted carbazole-fused DABNA derivative as an orange-red TADF emitter for OLEDs with nearly 40 % EQE. *Angew. Chem. Int. Ed.* **61**, e202212575 (2022).

[8] Yang, M., Park, I. S. & Yasuda, T. Full-color, narrowband, and high-efficiency electroluminescence from boron and carbazole embedded polycyclic heteroaromatics. *J. Am. Chem. Soc.* **142**, 19468–19472 (2020).

[9] Fan, X. C. *et al.* A quadruple-borylated multiple-resonance emitter with para/meta heteroatomic patterns for narrowband orange-red emission. *Angew. Chem. Int. Ed.* **62**, e202305580 (2023).

[10] Zeng, X. *et al.* Orbital symmetry engineering in fused polycyclic heteroaromatics toward extremely narrowband green emissions with an FWHM of 13 nm. *Advanced Materials* **35**, e2211316 (2023).

[11] Curtarolo, S. *et al.* The high-throughput highway to computational materials design. *Nat. Mater.* **12**, 191–201 (2013).

[12] Hansen, K. *et al.* Machine learning predictions of molecular properties: Accurate many-body potentials and nonlocality in chemical space. *J. Phys. Chem. Lett.* **6**, 2326–2331 (2015).

[13] Nakata, M. & Shimazaki, T. Pubchemqc project: a large-scale first-principles electronic structure database for data-driven chemistry. *J. Chem. Inf. Model.* **57**, 1300–1308 (2017).

[14] Ye, W., Chen, C., Wang, Z., Chu, I.-H. & Ong, S. P. Deep neural networks for accurate predictions of crystal stability. *Nature communications* **9**, 3800 (2018).

[15] Ju, C.-W., Bai, H., Li, B. & Liu, R. Machine learning enables highly accurate predictions of photophysical properties of organic fluorescent materials: Emission wavelengths and quantum yields. *J. Chem. Inf. Model.* **61**, 1053–1065 (2021).

[16] Xu, S. *et al.* Self-improving photosensitizer discovery system via bayesian search with first-principle simulations. *J. Am. Chem. Soc.* **143**, 19769–19777 (2021).

[17] Joung, J. F. *et al.* Deep learning optical spectroscopy based on experimental database: potential applications to molecular design. *JACS Au* **1**, 427–438 (2021).

[18] Cheng, Z. *et al.* Automatic screen-out of Ir (III) complex emitters by combined machine learning and computational analysis. *Adv. Opt. Mater.* **11**, 2370069 (2023).

[19] Gomez-Bombarelli, R. *et al.* Design of efficient molecular organic light-emitting diodes by a high-throughput virtual screening and experimental approach. *Nat. Mater.* **15**, 1120–1127 (2016).

[20] Cai, W. *et al.* Machine-learning-assisted performance improvements for multi-resonance thermally activated delayed fluorescence molecules. *Phys. Chem. Chem. Phys.* **26**, 144–152 (2024).

[21] Miao, N., Zhou, H., Mou, L., Yan, R. & Li, L. *Cgmh: Constrained sentence generation by metropolis-hastings sampling*, Vol. 33, 6834–6842 (2019).

[22] Xie, Y. *et al. Mars: Markov molecular sampling for multi-objective drug discovery* (2021). URL https://openreview.net/forum?id=kHSu4ebxFXY.

[23] Fan, X. *et al.* RGB thermally activated delayed fluorescence emitters for organic light-emitting diodes toward realizing the BT.2020 standard. *Adv. Sci.* **10**, e2303504 (2023).

[24] Gilmer, J., Schoenholz, S. S., Riley, P. F., Vinyals, O. & Dahl, G. E. *Neural message passing for quantum chemistry*, 1263–1272 (PMLR, 2017).

[25] Chibante, R. *Simulated annealing: theory with applications* (BoD–Books on Demand, 2010).

[26] Andrieu, C., De Freitas, N., Doucet, A. & Jordan, M. I. An introduction to MCMC for machine learning. *Machine learning* **50**, 5–43 (2003).

[27] Neal, R. M. *et al.* Mcmc using hamiltonian dynamics. *Handbook of markov chain monte carlo* **2**, 2 (2011).

[28] Zhou, G. *et al. Uni-mol: A universal 3d molecular representation learning framework* (2023). URL https://openreview.net/forum?id=6K2RM6wVqKu.

[29] Vaswani, A. *et al.* Attention is all you need. *Proc. Adv. Neural Inf. Process. Syst.* **30**, 6000–6010 (2017).

[30] Brookes, D., Park, H. & Listgarten, J. *Conditioning by adaptive sampling for robust design*, 773–782 (PMLR, 2019).

[31] Fannjiang, C. & Listgarten, J. Is novelty predictable? *CSH Perspect. Biol.* **16**, a041469 (2024).

[32] Omee, S. S., Fu, N., Dong, R., Hu, M. & Hu, J. Structure-based out-of-distribution (ood) materials property prediction: a benchmark study. *npj Computational Materials* **10**, 144 (2024).

[33] Li, Q., Miklaucic, N. & Hu, J. Out-of-distribution materials property prediction using adversarial learning based fine-tuning. *arXiv preprint arXiv:2408.09297* (2024).

[34] Fannjiang, C. & Listgarten, J. Autofocused oracles for model-based design. *Proc. Adv. Neural Inf. Process. Syst.* **33**, 12945–12956 (2020).

[35] Van der Maaten, L. & Hinton, G. Visualizing data using t-SNE. *J. Mach. Learn. Res.* **9**, 2579–2605 (2008).

[36] Ertl, P. & Schuffenhauer, A. Estimation of synthetic accessibility score of drug-like molecules based on molecular complexity and fragment contributions. *J. Cheminformatics* **1**, 8 (2009).

[37] RDKit: Open-source cheminformatics. http://www.rdkit.org. [Online; accessed 11-April-2013].

[38] Park, I. S., Min, H. & Yasuda, T. Ultrafast triplet-singlet exciton interconversion in narrowband blue organoboron emitters doped with heavy chalcogens. *Angew. Chem. Int. Ed.* **61**, e202205684 (2022).

[39] Yang, M. *et al.* Wide-range color tuning of narrowband emission in multi-resonance organoboron delayed fluorescence materials through rational imine/amine functionalization. *Angew. Chem. Int. Ed.* **60**, 23142–23147 (2021).

[40] Sriyab, S. *et al.* Photophysical properties of 1-pyrene-based derivatives for nitroaromatic explosives detection: Experimental and theoretical studies. *J. Lumin.* **203**, 492–499 (2018).

[41] Du, C.-Z. *et al.* Indole-fused bn-heteroarenes as narrowband blue emitters for organic light-emitting diodes. *J. Mater. Chem. C* **11**, 2469–2474 (2023).

[42] Zhang, Y. *et al.* Fusion of multi-resonance fragment with conventional polycyclic aromatic hydrocarbon for nearly bt.2020 green emission. *Angew. Chem. Int. Ed.* **61**, e202202380 (2022).

[43] Li, D. *et al.* High-performance narrowband oled with low efficiency roll-off based on sulfur-incorporated organoboron emitter. *Advanced Optical Materials* **11**, 2301084 (2023).

[44] Lu, T. & Chen, F. Multiwfn: a multifunctional wavefunction analyzer. *J. Comput. Chem.* **33**, 580–592 (2012).

[45] Naveen, R. K., Yang, H. I. & Kwon, J. T. Double boron-embedded multiresonant thermally activated delayed fluorescent materials for organic light-emitting diodes. *Commun. Chem.* **5**, 149 (2022).

[46] Liu, Z., Lu, T. & Chen, Q. An sp-hybridized all-carboatomic ring, cyclo[18]carbon: Electronic structure, electronic spectrum, and optical nonlinearity. *Carbon* **165**, 461–467 (2020).

[47] Joung, J. F., Han, M., Jeong, M. & Park, S. Experimental database of optical properties of organic compounds. *Sci. Data* **7**, 295 (2020).

[48] Riniker, S. & Landrum, G. A. Better informed distance geometry: Using what we know to improve conformation generation. *J. Chem. Inf. Model.* **55**, 2562–2574 (2015).

[49] Halgren, T. A. Merck molecular force field I basis form scope parameterization and performance of MMFF94. *J. Comput. Chem.* **17**, 490–519 (1996).

[50] Shuai, Z. Thermal vibration correlation function formalism for molecular excited state decay rates. *Chinese J. Chem.* **38**, 1223–1232 (2020).

[51] Frisch, M. J. *et al.* Gaussian˜16 Revision C.01 (2016). Gaussian Inc. Wallingford CT.

Acknowledgements

This research is supported by the National Science and Technology Major Project (Grant No. 2022ZD0117502) and the National Natural Science Foundation of China (Grant No. 22073055). This paper is also sponsored by Beijing Nova Program (20240484682). The authors thank Prof. Qiang Shi from the Institute of Chemistry, Chinese Academy of Sciences and Center of High Performance Computing, Tsinghua University for providing computational resources.

Author contributions

D.W. and H.Z. conceived the research. W.M., J.Z., L.D., D.W. and H.Z. co-supervised the project. M.P., T.T. and Y.O. designed the research. M.P. programmed the codes of MEMOS. T.T. conducted the DFT calculations. Y.O. trained the Uni-Mol models. Q.J. gathered and calibrated the experimental data of wavelengths and FWHM. Y.C. built a website showcasing the molecules generated by MEMOS. M.P. and T.T. drafted the original manuscript, including result analysis and visualization with the contributions of Y.O. M.P., T.T., D.W., and H.Z. conducted the manuscript editing and revision. All authors reviewed the final manuscript.